

## RECOMMENDATION ITU-R S.1061\*

**Utilization of fade countermeasures strategies  
and techniques in the fixed-satellite service**

(1994)

The ITU Radiocommunication Assembly,

*considering*

- a) that pressure on the limited RF spectrum from the increased demand for satellite services is leading to the use of higher frequency bands;
- b) that one of the major drawbacks associated with higher frequency satellite systems is the large signal attenuation caused by rain;
- c) that satellite channel performance as set forth in Recommendations ITU-R S.353, ITU-R S.522, ITU-R S.614 and ITU-R S.579 may be difficult to be achieved, in an economic way, by resorting only to power margin;
- d) that several systems have been developed to cope with rain attenuation whose performance and complexity are such that their applicability depends on the particular type of network involved,

*recommends*

**1** that the material contained in Annex 1 should give guidance for planning the utilization of fade countermeasure techniques in the fixed-satellite service.

NOTE 1 – It should be noted that the subject techniques may even be used in combination provided that no basic incompatibility exists among them.

## ANNEX 1

**Fade countermeasures in satellite communication systems****1 Site diversity operation****1.1 General design considerations**

The performance required for diversity earth stations is decided not only by the rain climate but also by the diversity configuration. The first kind of configuration is balanced diversity (diversity by two earth stations with equal performance). The other configuration is unbalanced diversity. In this configuration, the performance of one earth station (main station) is made sufficiently high, so that

---

\* Radiocommunication Study Group 4 made editorial amendments to this Recommendation in 2001 in accordance with Resolution ITU-R 44 (RA-2000).

the performance requirements of the other station (sub-station) may be considerably reduced. Such an unbalanced diversity configuration is expected when the main station antenna is equipped with a multiple-frequency band feeds such as 6/4 GHz and 14/11 GHz, and/or when the sub-station has to be simplified for technical and operational reasons.

Table 1 summarizes the results of sample calculations of the antenna diameter and the maximum transmit power required for balanced diversity links with low elevation angles. Estimates are given for two assumed diversity links: (A) Yamaguchi-Hofu (diversity distance = 20 km) and (B) Yamaguchi-Hamada (100 km); both in Japan.

It is seen from this Table that the antenna diameters required for the 14/11 GHz FM link (14 GHz for uplink and 11 GHz for downlink) are about 28 m and 19 m for cases (A) and (B), respectively. When the diameter of the main station can be made larger than those values, the required diameter for the sub-station becomes smaller. Values shown in this Table are derived using many of the link parameters established for Intelsat-V satellites, so they are subject to change when the link parameters are different from those used here.

TABLE 1

**Sample calculations of the required performances for balanced diversity links with low elevation angles (14/11 GHz)**

Location	(A) Yamaguchi-Hofu		(B) Yamaguchi-Hamada	
Elevation angle (degrees)	9.1	9.1	9.1	8.4
Diversity distance (km)	20		100	
FM				
Required antenna diameter (m)	28/32		19/22	
Required transmit power <sup>(1)</sup> (W) (maximum value)	730		510	
TDMA <sup>(2)</sup>				
Required antenna diameter (m)	17/19		11/12	
Required transmit power (W) (maximum value)	530		400	

(1) Values for 792 channel FDM-FM carrier (25 MHz).

(2) Values for 4-phase CPSK at 120 Mbit/s with forward error-correction.

*Assumptions :*

Frequency: 14.5 (uplink)/11.7 (downlink) GHz

Orbital position of satellite: 63° E, 0° N

Satellite e.i.r.p.: 41.1 dBW

Antenna diameters are estimated for two cases, namely:

$$T_s = 50 \text{ K and } T_s = 150 \text{ K}$$

$T_s$ : system noise temperature of the earth-station antenna

Efficiency of the earth-station antenna: 65%

Estimates are based on the rain-rate statistics obtained for those locations.

The calculation methods of the required performances (antenna diameter and e.i.r.p.) for the diversity earth stations are different depending on the diversity configurations. In the design of a balanced diversity link, calculations have to be based upon the joint probability distribution of the rain attenuation at both locations, while in the case of an unbalanced diversity configuration, the cumulative time distribution of the rain attenuation and the conditional probability of the attenuation are required.

The conditional probability  $P(L''/L')$  is the probability with which the rain attenuation at the site of the sub-station exceeds  $L''$  under the condition that the rain attenuation at the main site exceeds  $L'$ .

In order to perform reliable estimates of the earth station requirements, reliable statistics on the basis of the long-term propagation measurements are needed.

## 1.2 Site diversity switch-over operation

To implement diversity earth stations, care should be exercised on the switch-over operation, because, in the event of switch-over, short duration signal loss or overlap may occur due to the difference in path length of diversity routes or carrier phase discontinuity.

In analogue transmissions such as FM-FDMA, switch-over in transmitting will necessarily cause discontinuity of carrier phase which will result in a signal transient at the demodulator output in the receiving earth stations. Signal transients due to switch-over at the receive earth station may be avoided by carefully adjusting the electrical path length of each diversity link measured from the switch-over equipment to the satellite.

In digital transmissions it is possible to avoid signal transients even in the event of switch-over at the transmit earth station by providing dummy intervals in the transmitting signal sequence and making the switch-over during the dummy interval. In the receiving earth stations the dummy intervals should be discarded whether or not switch-over took place.

Transient switch-over both in the transmitting and receiving of the diversity system may most conveniently be achieved in TDMA transmission. The dummy intervals are built-in because TDMA transmission occupies only a part of the TDMA frame. Furthermore, TDMA demodulators are capable of receiving burst mode carriers of incoherent phase. Therefore, phase incoherency of TDMA carriers does not cause any difficulty. The only possible problem of site diversity operation of TDMA transmission would be the necessity of very precise transmit timing control even for the initial transmission from the stand-by station. This may be solved either by continuously transmitting a dummy burst from the stand-by station or by obtaining sufficiently accurate ranging data of the satellite which is possible when the TDMA system employs open loop synchronization. In TDMA transmission, the path lengths of diversity routes can be equalized using the reception timing of frame synchronization signals. The reception timing of signals from both diversity routes can be automatically equalized by controlling the variable delay line inserted in one of the diversity routes. An experimental system using the dummy burst technique has been tested.

For route selection in diversity operation, it is necessary to measure the transmission quality of diversity routes. Because the diversity effect may degrade depending on the choice of the measuring method of link quality, care should be taken on selecting the measuring time duration and achievable accuracy.

### 1.3 Diversity interconnect link

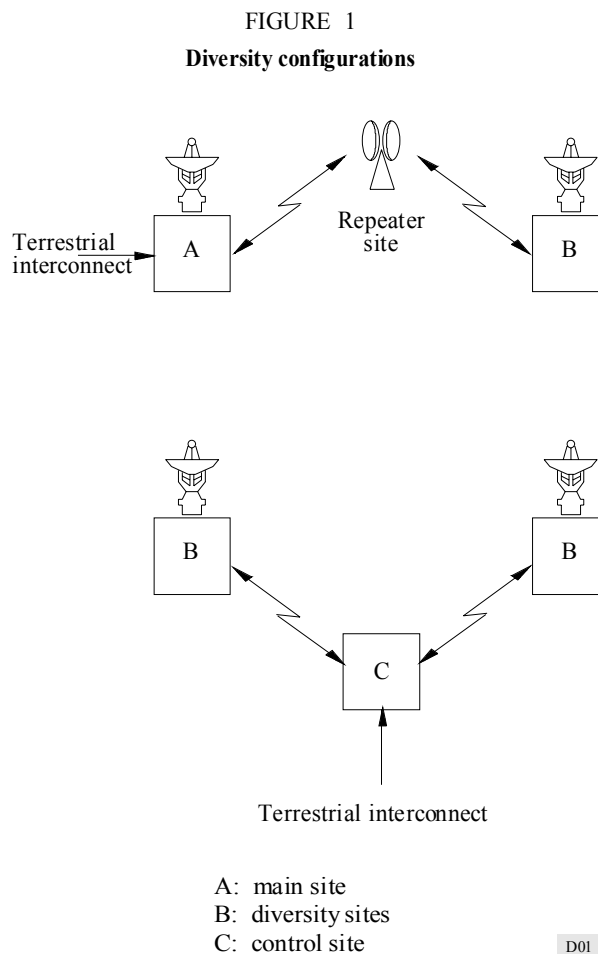
A factor which must be considered is that the ITU-R hypothetical reference circuit contained in Recommendation ITU-R S.352 and the ITU-R hypothetical reference digital path contained in Recommendation ITU-R S.521 include the diversity interconnection links (DIL) to the diversity switching point and any additional modulation/demodulation equipment required. This would mean that system noise budgets must include all the effects of the DIL.

#### 1.3.1 Basic configuration

##### 1.3.1.1 Physical aspects

There are a number of different specific configurations which can be considered and there could be reasons for preferring one of these. Two of these are identified and described in this Annex as (see Fig. 1):

- a main site which contains the diversity switch and the terrestrial interface. The diversity site is connected by a two-hop microwave DIL using either an active, or passive, repeater. (A repeater site is assumed, since the likelihood of mutual visibility of the diversity sites is small);
- dual diversity sites and a separate control site with the interface and diversity switch; single microwave hops for each site to the control site.



It may also be possible to employ cable or waveguide links for the DIL. When both FDM-FM and TDM (FDMA or TDMA) are used at an earth station, two parallel links would usually be required.

### **1.3.1.2 Modulation requirements**

When FDM-FM is used, remodulation will be required because the satellite link modulation and baseband configurations are usually different from those conventionally used for terrestrial systems. The main difference is associated with the channel packaging. The terrestrial system will usually combine the channels in one or more basebands in each direction and will use a relatively low modulation index. The earth station will break these basebands down into multiple, multi-destination, transmit basebands; different from those on the terrestrial system and using a different modulation index. The receive basebands are even more numerous and may consist of only a few channels and these must be re-combined into the terrestrial basebands. This process requires modulation/demodulation equipment at the main earth station site and at the diversity site where conventional design of the DIL is used. All configurations can be implemented using the remodulation technique at the expense of providing duplicate equipment at the diversity site.

An alternative technique is to use the same modulation arrangements on the terrestrial system as used on the satellite system. Such a technique would appear to be technically feasible although not conventional. The incentive is to save the cost of remodulation equipment at perhaps some added cost to the terrestrial system, although savings may also result for this element as well. The use of such a technique is only applicable to the second configuration of Fig. 1. When TDM is used (FDMA or TDMA), either technique could be employed. In the case of TDMA, diversity switching is performed between bursts (see § 1.2). The same modulation could be used on the DIL as used on the satellite system although the data rates would not normally be those of a conventional terrestrial digital radio system.

## **1.3.2 Technical factors**

### **1.3.2.1 Frequency selection**

Frequency selection for a microwave DIL requires careful study to ensure that the required overall performance is obtained. Information on terrestrial microwave propagation is shown in the relevant texts of Radiocommunication Study Group 3.

### **1.3.2.2 Bandwidth requirements**

The bandwidth required to implement the DIL can be related to the earth station bandwidth by a factor which may be unity or less, depending upon whether re-modulation is used or not. If only frequency translation is used then bandwidth requirements must be MHz for MHz. By re-modulating, a greater channel density can be achieved by using smaller FM modulation indices at the expense of a substantial multiplex interface.

### 1.3.2.3 Rain attenuation

Further factors are rain attenuation and site diversity characteristics which are both related to rainfall phenomenon. A dry climate is preferred. Diversity action is a function of the site spacing. It is expected that the nominal spacing required is about 16 km. The best orientation of a line connecting the sites may be assumed to be perpendicular to the direction of predominant weather patterns since the most severe attenuation condition would not be expected to affect both sites simultaneously and maximum diversity action would be obtained. The weather effects on the microwave DIL must be accounted for if the higher frequencies are used for these links, although this should be a secondary consideration.

### 1.3.2.4 Variations in transmission delay due to diversity switching

Another element of importance is associated with the differential transmission delay between the diversity signals as they arrive at the switching point.

## 1.3.3 General considerations

Two particular aspects of the diversity interconnection links (DIL) are important:

- the contribution to the overall system noise budgets, and
- the contribution to system outage.

These subjects are studied here to develop the effects of the important parameters and the interrelationship with the satellite link parts of the system.

The diversity link design can be made on two bases. If a re-modulation system is selected, then conventional radio-relay designs can be used. If a translation system is selected, then the design can follow a different pattern and will be very similar to the satellite system transmission design. Fading margins and noise contributions must be accounted for in overall performance. In the special case where the same frequencies are used for the DIL as for the satellite system, then interference noise allowances must also be made.

### 1.3.3.1 Noise budgets for FDM-FM

The contributions of the DIL to the overall noise of the hypothetical reference circuit have to be made reasonably small in order to maintain the system performance in accordance with Recommendation ITU-R S.353.

It seems reasonable to assume that the DIL noise contribution would be considered as part of the earth station budget (usually 1 500 pW0p), as the DIL actually provides part of the normal earth station function. It only needs to be determined that such a contribution can be kept sufficiently small so that the total of 1 500 pW0p is not exceeded. The fading of the DIL will contribute to the overall short-term noise budget of the link.

The noise contribution from the DIL would have a number of components depending upon the implementation configuration and the frequency bands used. The components are:

a) *Thermal noise*

Conventional ITU-R designs for radio-relay are 1 to 3 pW0p per km or less, and can be held to 10 pW0p or less, for a single hop. Special designs also achieve small contributions. The time

varying components due to multipath fading and rain attenuation are relatively large, but for short hops can be controlled to reasonable values. The thermal noise is related dB for dB to the fading from either mechanism.

b) *Basic intrinsic noise*

This is baseband noise and is applicable only to re-modulating configurations. Noise levels of 50 to 100 pW0p are usual for back-to-back basebands. The normal earth station noise budget provides for one such contribution while a re-modulation configuration would add a second contribution.

c) *Interference*

A very small interference contribution would be present from other microwave systems operating in the same frequency bands in some cases. This contribution can be considered to be negligible. For the special case of using the same frequency re-use design, uplink and downlink contributions of interference at the earth station can be expected. Values of the order of 10 to 100 pW0p are estimated for normal operation. In addition, certain fading situations may be accompanied by increases in this noise for very short time periods along with the thermal noise. This configuration does not require re-modulation, so all extra noise associated with item b) is eliminated.

d) *Intermodulation*

A re-modulating design will have an extra modulator-demodulator pair plus IF amplifiers, while the translation design is all conventional earth station equipment and therefore contributes very little intermodulation noise.

Table 2 illustrates a possible noise budget:

TABLE 2

Sample budgets – Free space conditions				
	Re-modulation (2 hops)		Frequency translation (1 hop)	
	Low (pW0p)	High (pW0p)	Low (pW0p)	High (pW0p)
Thermal	2	20	1	10
Baseband intermodulation	50	100	–	–
Interference	–	–	10	100
Intermodulation (RF)	100	200	20	50
Total (pW0p)	152	320	31	160

### 1.3.3.2 Error budget for TDMA

The contributions of the DIL to the overall error rate of the hypothetical digital reference path have to be made reasonably small in order to maintain the system performance in accordance with this Recommendation.

It should be noted that in the case of the re-modulating DIL the errors will be additive whereas in the case of frequency translation the noise effects will be additive.

### 1.3.3.3 Frequency considerations

The fading characteristics as a function of frequency, climate and path length for rainfall can be derived from conventional microwave designs. Rain attenuation and multipath fading are independent events – in fact they are almost mutually exclusive.

Since the expected spacing of a diversity pair of earth stations is of the order of 16 to 24 km and since it is also expected that either a repeater or a common site will be needed, the individual path lengths of the DIL will probably not exceed 16 km. The margins for such a path length can normally be made sufficiently high to accommodate short-term outages as low as 0.001% of the time.

## 2 Uplink transmitting power control

### 2.1 Introduction

Uplink power control (UPC) can be used as a means of reducing the effect of uplink attenuation in the higher frequency bands (for example 14/11 and 30/20 GHz bands). This technique could be used to achieve efficient operation of a satellite communication system and to decrease interference to other satellite and terrestrial links by reducing clear-sky e.i.r.p.

### 2.2 Implementation of UPC

There are various methods of achieving UPC. The most commonly used methods are as follows.

#### 2.2.1 Open-loop UPC method

Open-loop UPC is a method whereby a beacon signal from the satellite is used to measure the downlink rain attenuation. Owing to the correlation between the uplink and downlink rain attenuation, this measurement is used to estimate the uplink rain attenuation level and hence the UPC control values. Most predicted attenuation values coincide with actual values; however, some values differ because of such environmental conditions as wind velocity or raindrop-size distribution. Table 3 shows an example of potential errors in estimating uplink (14 GHz) attenuation from a downlink (11 GHz) measurement.

Some potential error sources have been excluded as being too small to estimate (e.g. antenna tracking error, satellite antenna pointing error, pre-emphasis error, antenna gain degradation, refractive effect at low elevation angles, rapid rainfall rate fluctuation). Also excluded are error



sources of a very rare type (e.g. large accumulations of wet snow on the antenna, failure in the control or measurement circuits). Various combinations of these additional error sources could, potentially, make the cumulative uplink power level error larger.

TABLE 3

**Example of potential errors in estimating uplink (14 GHz) attenuation from a downlink (11 GHz) measurement is tabulated below**

a) Uplink attenuation of less than 1.0 dB			
	Elevation angle		
	5°	15°	25°
Equipment error <sup>(1)</sup>	0.725	0.725	0.725
Ice attenuation	0.05	0.05	0.05
Water vapour/diffusive	0.20	0.10	0.05
Clear-sky level	0.10	0.10	0.10
Maximum uplink error (dB)	±1.075	±0.975	±0.925
b) Uplink attenuation of between 1 and 6 dB			
	Elevation angle		
	5°	15°	25°
Equipment error <sup>(1)</sup>	0.725	0.725	0.725
Ice attenuation	0.05	0.05	0.05
Raindrop-size distribution	0.10	0.075	0.05
Water vapour/diffusive	0.20	0.10	0.05
Clear-sky level	0.10	0.10	0.10
Polarization error	0.10	0.075	0.05
Path length error	0.20	0.10	0.05
Melting layer	0.05	0.05	0.05
Maximum uplink error (dB)	±1.525	±1.275	±1.125
c) Uplink attenuation in excess of 6 dB			
	Elevation angle		
	5°	15°	25°
Equipment error <sup>(1)</sup>	0.725	0.725	0.725
Ice attenuation	0.05	0.05	0.05
Raindrop-size distribution	0.20	0.15	0.10
Water vapour/diffusive	0.10	0.075	0.05
Clear-sky level	0.10	0.10	0.10
Polarization error	0.20	0.15	0.10
Path length error	0.40	0.25	0.15
Melting layer	0.05	0.05	0.05
Maximum uplink error (dB)	±1.825	±1.550	±1.325

<sup>(1)</sup> The equipment error of ±0.725 dB assumed above is estimated on the basis of a ±0.5 dB error being encountered at 11.7 GHz (on the downlink) and assuming a 1.45 scaling factor between 11.7 GHz and 14 GHz. The ±0.5 dB error was obtained using available data and needs further verification by additional measurements.

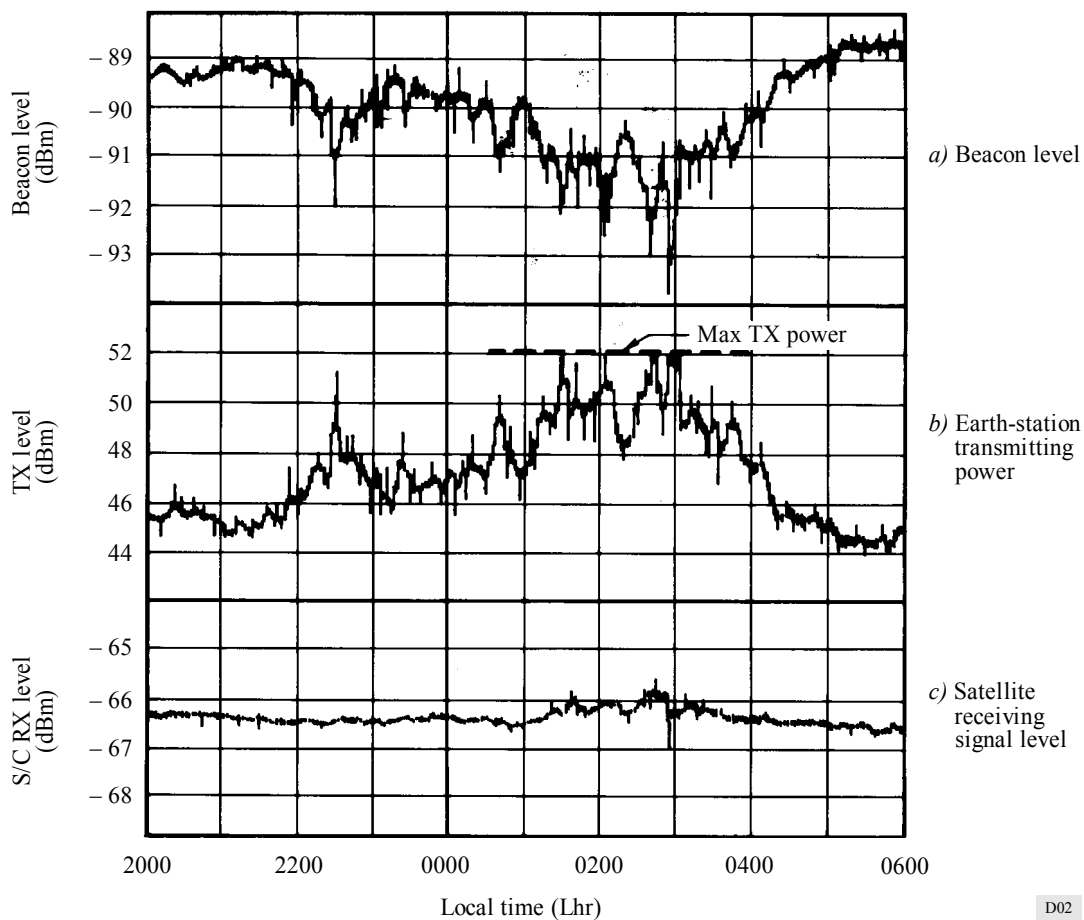
### 2.2.2 Closed-loop UPC method

Closed-loop UPC is a method whereby the beacon signal from the satellite is compared with the loop-back  $C/N$  or  $S/N$  of a pilot signal or special channel signal. In this way the uplink rain attenuation and the UPC control value can be determined with high accuracy. A disadvantage of the approach, however, is that separate control channels in addition to the communication channel are necessary.

### 2.3 Uplink power control (UPC) experiment

An open-loop UPC experiment was conducted using the 30/20 GHz band with the result shown in Fig. 2. In this experiment, the UPC values were determined from the values of downlink attenuation. Fig. 2a) shows the beacon level, Fig. 2b) the HPA transmitting power level, and Fig. 2c) the satellite receiving level. As shown, the variation in total  $C/N$  values can be kept within 1 dB (peak-to-peak) except in the period in which the required transmitting power exceeds the maximum transmitting power.

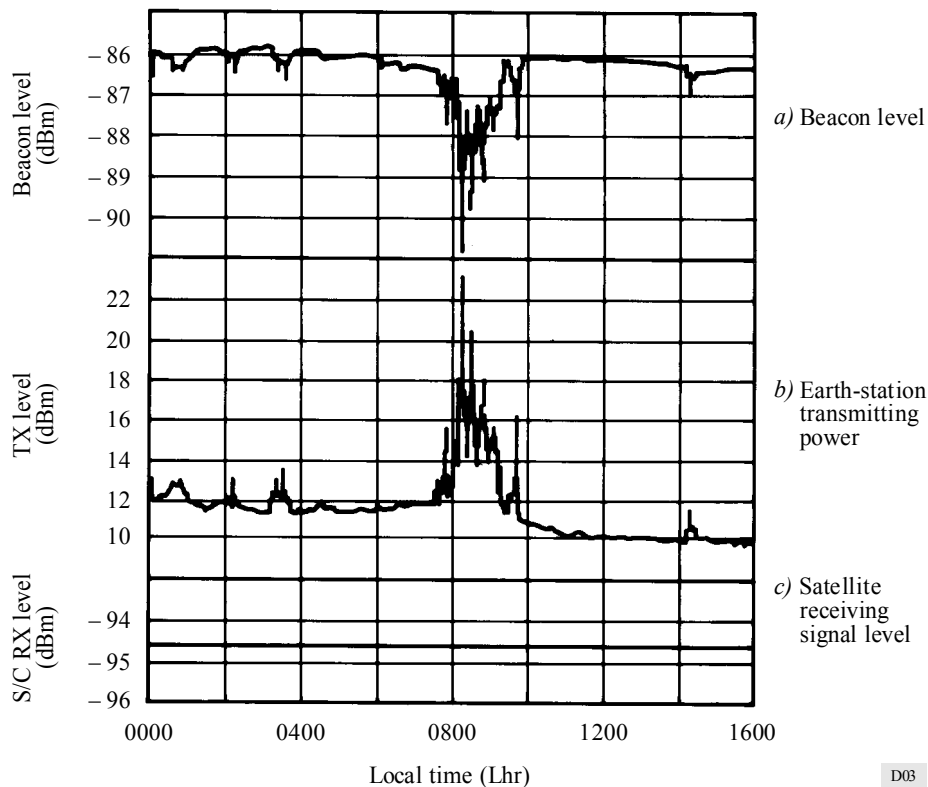
FIGURE 2  
Experimental results of open-loop UPC



D02

A closed-loop UPC experiment was also conducted using the 30/20 GHz band with the result shown in Fig. 3. The control error was kept within 0.3 dB (peak-to-peak).

FIGURE 3  
Experimental result of closed-loop UPC



## 2.4 Open-loop UPC using a radiometer

Uplink power control can be achieved by using a radiometer to measure the energy emitted by rain along the propagation path to the satellite. No beacon or pilot signal is required. Errors introduced by beacon receivers, such as the variation of gain with LNA temperature, etc., are eliminated.

The relationship between slant-path precipitation attenuation and antenna temperature has been examined by several investigators. Path attenuations calculated from measurements of the antenna temperature are generally accurate to better than 0.5 dB for attenuations less than 6 dB (at 12 GHz, in Canada). In a practical system, the uplink power will not likely be increased appreciably more than 6 dB. Thus, the radiometer can be used to compute path attenuations over the entire range of practical interest.

Sun transits will occur for a few days near the equinoxes when the declination of the Sun is approximately that of the satellite. To distinguish between these increases in antenna temperature and those due to rain attenuation at other times, the satellite and solar look angles are calculated frequently. When the angular separation between the radiometer antenna axis and the Sun is less than a chosen angle, the increase in antenna temperature is assumed to be due to the Sun and uplink power control is inhibited.

An uplink power control system has been developed for the 14/12 GHz band in which a radiometer measures the antenna temperature in a band of frequencies below the uplink band, calculates the path attenuation at the desired uplink frequency and controls the signal strength applied at IF to the up-converter. The antenna temperature is measured by a new type of radiometer. The principle of operation differs fundamentally from that of the conventional Dicke radiometer and results in a very stable measurement of antenna temperature. The entire radiometer is contained within a cylinder mounted at the prime focus of a parabolic reflector. The radiometer frequency must differ from the uplink frequency so that transmitted energy which is backscattered from rain along the path is not detected by the radiometer, a radiometer frequency of 13.3 GHz is used.

In an experiment using the system described above, the loopback signal strength was compared with the received signal strength of the satellite beacon. The signal strengths were well correlated, indicating that the uplink signal strength as received at the satellite was almost constant, independent of rain attenuation. Additional operational experience will be gained with the two uplink power control systems currently being installed in Canada.

## **2.5 Conclusion**

UPC is one of the most important techniques for establishing higher frequency band satellite communications systems. By using UPC for the higher frequency bands, interference between neighbouring satellite systems and terrestrial networks can be reduced. As a result, efficient utilization of the geostationary-satellite orbit and efficient system operations can be achieved.

Detailed studies will be necessary for more accurate UPC methods.

## **3 Variable transmission systems**

### **3.1 Introduction**

System performance of digital satellite communication systems can be improved by reducing adaptively the information transmission rate during poor propagation conditions. Variable parameters (clock rate and number of phase states) of PSK modulation and the variable coding rate of FEC (forward error correction) can be used for variable information transmission rate. A synchronization sum method for a demodulated PSK signal has also been applied to a variable transmission rate TDMA system.

It should be noted that public services may not be able to be subjected to reduction in information rate, and that other fade countermeasures may be necessary in these cases.

### **3.2 Variable parameter system of PSK modulation**

Various kinds of general purpose PSK modems have been developed using LSI type digital signal processors. These modems have two modes of operation, BPSK and QPSK, and their transmission clock rates are continuously variable. They are suitable for a variable transmission rate system although high transmission rates are not achievable because of the limitation on operational speed of the digital signal processor. For example, a modem with a maximum transmission rate of

400 kBd has been developed. This modem can be applied to a burst mode signal. In another example, a modem with a maximum transmission rate of 6 MBd has been developed. This transmission rate is variable, but it takes a significant amount of time to reach a stable state after resetting the parameters.

When the reduction ratio of the transmission rate is  $\gamma$ , improvement of  $C/N$  is given by:

$$\Delta(C/N) = -10 \log \gamma \quad \text{dB}$$

### 3.3 Variable coding rate system

Convolutional encoders and Viterbi decoders are suitable for a variable coding rate system because these codecs are expected to be constructed economically in the form of LSI and their coding gains are high. For example, LSI type codecs of constraint length = 4 or 7, coding rate = 1/2 or 2/3 or 3/4 or 7/8, and maximum transmission rates = 20 to 25 MHz have been developed. One of these is a general purpose codec with a selectable coding rate.

$C/N$  improvement, when a codec is applied to the variable information transmission rate system, is given as:

$$\Delta(C/N) = 10 \log (R_o/R_a) + G_a - G_o \quad \text{dB}$$

where:

$R_o$ : coding rate

$G_o$ : coding gain at operation in clear sky conditions

$R_a, G_a$ : same as above for operation in rain conditions.

### 3.4 Variable transmission rate system using spread spectrum and synchronization sum techniques

There is another method which falls within the variable transmission rate category. A baseband data bit stream (information bits or error correcting bits) is scrambled by a constant clock rate PN code and then PSK modulated. The transmission rate can be varied by changing the ratio of the data bit rate and the clock rate of the PN code. The selected ratio must be  $1/n$  where  $n$  is a positive integer. In a receiver, the scrambled signal is PSK demodulated at the clock rate of the PN code and despread by the PN code. After synchronization of the PN code, the baseband data bits are detected.

This technique has been applied to a variable transmission rate TDMA system in which the transmission rate is adaptively variable at each TDMA burst. It has been confirmed by experiments that the degradation of bit error rate performance, compared with theoretical performance in a Gaussian channel, is less than 2 dB when the TDMA system operates at a rate of  $8/n$  Mbit/s ( $n = 1, 2, 4, 8, 16, 32$ ).

This technique may be considered as modulation and demodulation capable of varying transmission rates using a constant clock or a variable coding rate with a coding gain of 0 dB.

### 3.5 Conclusion

Three kinds of variable information transmission rate techniques are discussed as methods of maintaining the signal quality of a digital satellite communication system during poor propagation conditions.

The variable coding rate technique using a convolutional encoder and a Viterbi decoder is suitable for a simple communication system with relatively economic and/or simple earth station equipment.

The other techniques are to be used in combination with a forward error correction technique. In the variable parameter system, however, an adaptively variable transmission rate modem with a maximum rate of more than 400 kBd has not been developed. The variable transmission rate technique using the synchronizing sum fits a TDMA system rather than an SCPC system.

## 4 Fade countermeasures using time division multiple access techniques (FCM-TDMA)

### 4.1 Introduction

FCM-TDMA is a method of countering the severe effects of precipitation at the higher frequencies; it is an adaptive system which allocates an additional time resource to fading carriers in a TDMA network to thus provide an acceptable error rate in the degraded  $C/N$  environment which occurs during fading.

A FCM-TDMA system has a portion of the frame designated as a shared resource, which is made available to fading carriers. This means that the frame efficiency, and therefore capacity, of a FCM-TDMA system is less than that of an equivalent conventional TDMA system under clear-sky conditions. The frame period is not normally a variable but any bursts suffering fading are expanded in time within the frame. This means that a burst retains the same number of information (user) bits when expanded, therefore the information rate is not changed. The technique is therefore particularly suited to public switched services/networks, where variable information rate techniques (see § 3) may not be appropriate.

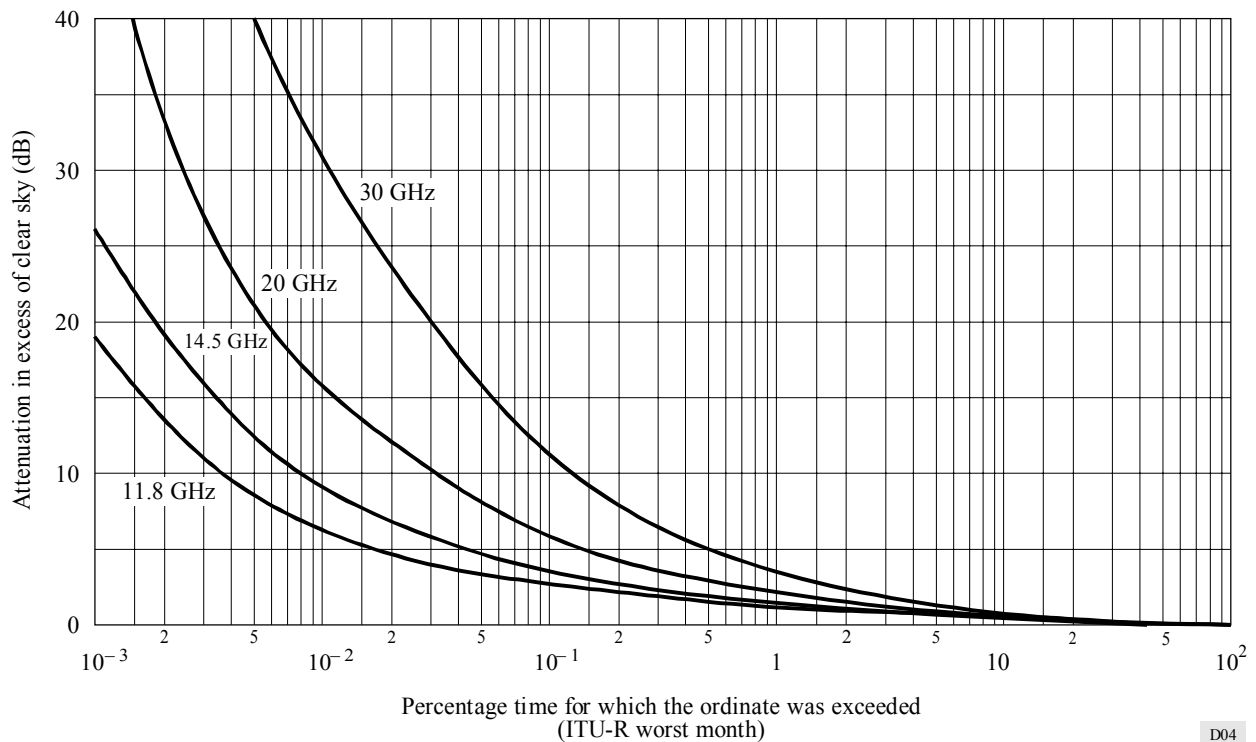
Each burst need only be expanded to the degree necessary to counter the fading experienced on a particular routing, be it on the uplink or downlink, or both to maximize the efficiency of the system.

### 4.2 Time space statistics of atmospheric fading at 30/20 GHz

A series of measurements was carried out over 43 months at Martlesham Heath, East Coast, United Kingdom (ITU-R climatic zone E) at 14/12 GHz on a 30° elevation path to the OTS2 satellite. The results of these measurements for the single site were scaled to 30/20 GHz using the ITU-R frequency scaling ratios and are summarized in Fig. 4, which gives the worst month attenuation statistics. Then, using this measured data, a computer model was developed for predicting statistics of simultaneous fading on two or more of the links throughout a satellite coverage area, assuming all links have access to the spare resources, in order to estimate the improvement in link availability which an adaptive-TDMA system would provide.

Simultaneous fading at  $n$  stations in a circular zone of diameter  $d$  was modelled by taking  $n$  time points from the (above-mentioned) measured database within time span  $t$  where  $t$  and  $d$  are related by a factor of 30 km/h i.e. the “effective” wind speed prevailing in the United Kingdom during periods of precipitation. Long-term statistics are then compiled by sliding this window of width  $t$  over the entire 43 month database, and converted to ITU-R worst month statistics.

FIGURE 4  
Typical curves of attenuation against single site availability  
(ITU-R worst month)



D04

Extensive work has been carried out to compare this model with direct measurements over known distances, and to check the validity of the 30 km/h conversion factor. Comparisons were made with:

- the Hodge model of site diversity (up to 10 km),
- rainfall rate correlations (up to 400 km),
- meteorological office data (up to 1 200 km).

There was fairly good agreement of the above-mentioned data/models with the model used and the conversion factor of 30 km/h for distances greater than 10 km.

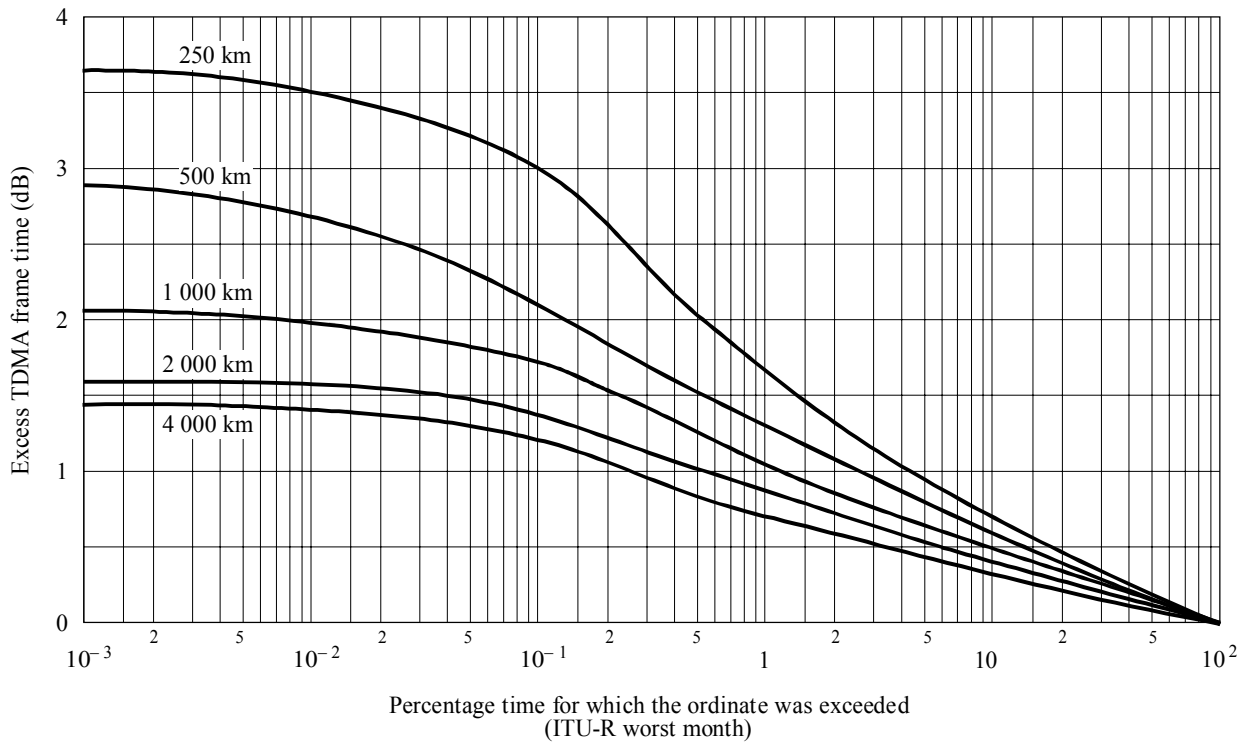
The model was used to compile statistics of the reserve TDMA frame time required at the satellite to maintain an adequate  $E_b/N_0$  on 20 GHz downlinks to hypothetical networks comprising various numbers of earth stations.

It was found that if the frame time in the reserve pool is sufficient to keep the outage of Fig. 5 well below 0.01%, then the overall outage will be dominated by the single site outage of Fig. 4.

Different uplink fade compensation techniques (such as rate variation) may be worthy of consideration depending upon the network topology.

FIGURE 5

Typical curves of excess satellite power against system availability



D05

### 4.3 Methods of using an expanded burst to provide a level of noise immunity

There are several ways of using the additional time provided by an extended time slot to give a greater degree of noise immunity, the following are examples:

a) *FEC*

Differing rates of FEC overhead can be introduced in stages with increase in fade depth, the time slot being extended as necessary.

b) *Reduction in transmitted data rate*

The transmitted data rate can be reduced and the same information rate conveyed by increasing the burst length. If the transmitted data rate is reduced, the noise bandwidth at the receiver can also be reduced, giving increased noise immunity.

c) *Replication of the user data within the burst*

A burst suffering fading can be repeated (replicated) a number of times, and a sophisticated demodulator employed to interpret the received signal by taking a mean value for each symbol.

The above techniques all have implications on the modem design and care must be taken to ensure clock and carrier synchronization is retained during a fade. Furthermore, if the symbol rate is changed (resulting in a variation of spectra and power flux-density between bursts), there may also be interference implications.



The depth of fade which can be countered varies according to the method employed and the degree of sophistication which can be built into the modem. In practice, a composite FCM-TDMA system may be preferable; for example, adaptive FEC could be used together with any of the other methods outlined, and there is a case for using permanent FEC with method c).

#### 4.4 System control

FCM-TDMA systems will need robust protocols and control mechanisms to identify the onset and level of fading on any routing, to determine which bursts need to be expanded and by how much, and to implement such expansions together with any time-plan revision.

#### 4.5 Conclusions

An FCM-TDMA system must be tailored to need. There are many system parameters which must be determined, for example, the maximum expansion which is to be given to any particular burst, the expansion step size, the implementation or reaction time to onset of fading, the percentage of the frame to be allocated as the shared resource, etc. The sizing of these parameters will depend on the nature of the network, the climatic region, the maximum depth of fade to be countered, and on the number and data rate mix of carriers.

It may also be possible to combine FCM-TDMA with other fade countermeasures systems; for example, the FCM-TDMA protocols could be developed to incorporate uplink power control, or FCM-TDMA could be combined with a frequency diversity system whereby bursts subject to severe fading are transmitted in an alternative TDMA frame at a lower frequency.

Extensive work has been carried out in the United Kingdom to model the “space-time” statistics and to demonstrate the feasibility of adaptive-TDMA using data replication methods. Although this would require operating the demodulator at very low  $E_b/N_0$  ratios during fades, experiments in one laboratory have been carried out successfully at  $E_b/E_0$  ratios down to  $-8$  dB. However, further work is needed in both the modelling and equipment areas to develop a practical system.

## 5 Frequency diversity technique

### 5.1 Introduction

Dual-band frequency diversity is an adaptive fade countermeasure to rain attenuation applicable in the case of satellites operating in two frequency bands, typically a high frequency band, such as 30/20 GHz band, and a low frequency band, such as 14/11 or 6/4 GHz band.

Normally the traffic is routed through the high frequency 30/20 GHz band, where a large bandwidth is available. When the power margin on a particular link operating in 30/20 GHz band is not sufficient to overcome rain attenuation, traffic on this link is switched to the lower frequency band, which is less affected by rain.

The reserve capacity available at the lower frequency band, that is shared among the stations that at a certain time would need protection against fading, is called here the shared resource or back-up band.

Dual-band frequency diversity provides a large equivalent power gain since, for a given total outage requirement, the acceptable outage time for the link using the high frequency band (30/20 GHz) is significantly increased, so that a much higher link attenuation is tolerable.

In general the use of a pool of back-up channels is an efficient solution, considering that on average the number of links requiring simultaneous back-up capacity is small.

A theoretical analysis of a frequency diversity system is performed in § 5.2, to evaluate the number of reserve channels needed to counteract fading in a satellite network.

In § 5.3 some problems arising in the design of the control system of the adaptive fading countermeasures are presented.

Finally, in § 5.4, the effects on the performance of different switchover procedures, obtained by simulating the system on the basis of the attenuation time series at 11.6 GHz, measured over four years, are presented.

## 5.2 System analysis

A satellite communication network of  $N$  stations is considered such as, for instance, a TDMA system operating normally at 30/20 GHz frequency band but with a back-up capacity available at a lower frequency band (14/11 or 6/4 GHz). Outage in the link between two stations A and B occurs when a fade larger than a specified threshold value is encountered either in A or B and at that moment no back-up capacity is available. This happens when the back-up channels have already been assigned to protect other faded links in such a way that no other request can be accommodated.

To evaluate the outage probability due to rain attenuation, the joint statistics of fades at the  $N$  station sites are needed. These depend upon the particular geographical configuration of the network. To develop a general analysis, we use a simple model.

The yearly averaged outage probability for a given station is denoted by  $p$  (even if not necessary,  $p$  is assumed equal for the  $N$  stations, for the sake of simplicity). The fact should be taken into account that fades at different sites are not in general statistically independent because of both time (seasonal) and space (geographical) correlation. It is assumed that the conditional probability of fading at station B (event  $F_B$ ), given that there is fading at station A (event  $F_A$ ), is not simply  $p$  as in the case of statistical independence, but is increased by a factor  $\alpha \beta$ :

$$P(F_B/F_A) = \alpha \beta p \quad (1)$$

The seasonal correlation factor is denoted by  $\alpha$  and  $\beta$  is the geographical correlation factor. The factor  $\beta$  can be assumed equal to unity when the stations A and B are very widely spaced, but otherwise it will be larger since correlation between rainfall at different sites may still exist among sites at hundreds of kilometres apart.

Generalizing (1), the joint probability of fading at stations 1, 2, ...,  $M$  conditioned by the event  $F_A$  can be expressed as:

$$P(F_1, F_2, \dots, F_M/F_A) = (\alpha \beta)^M P(F_1) \dots P(F_M) = (\alpha \beta p)^M \quad (2)$$

Based on this model, the evaluation of the outage probability at station A,  $P(OUT_A)$ , can be carried out by calculating the probability that no back-up capacity is available when fading occurs in A. If the back-up capacity consists of  $k$  back-up channels at a lower frequency band, the outage probability at a given station A can be derived using equation (2)

$$P(OUT_A) = p \sum_{j=k}^{N-1} \frac{j+1-k}{j+1} \binom{N-1}{j} (\alpha \beta p)^j (1 - \alpha \beta p)^{N-1-j} \quad (3)$$

where:

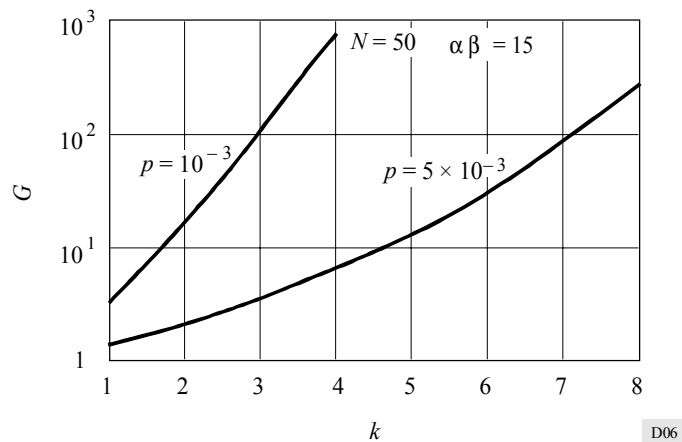
$k$ : total number of available back-up channels.

The factor  $(j+1-k)/(j+1)$  represents the probability that no back-up channel from the pool is assigned to A when  $j$  faded stations ( $j \geq k$ ), in addition to A, request a back-up channel. Note that the outage probability for the link (A, B) is approximately twice the outage probability at station A (or B) if the joint probability of fading at A and B is much lower than the probability of fading at A (or B). As an example, Fig. 6 shows the outage reduction factor (ratio between outage probability with frequency diversity and without) as a function of the number of back-up channels  $k$  for a particular case, namely for  $N=50$  and  $\alpha \beta = 15$ . The curves correspond to two values of  $p$ , the outage probability when the system is not protected with frequency diversity. The probability  $p$  depends on the built-in power margin at the station transmitter. The probability for a given attenuation  $A$  to be exceeded depends on the frequency as well as on the meteorology of each station site. For the calculations in the example the following attenuation versus cumulative distribution function was assumed:

$$A = A_{0.01} 0.12p^{-(0.546 + 0.043 \log p)} \quad \text{dB} \quad (4)$$

where  $p$  is the probability (in percentage for an average year) for the attenuation  $A$  to be exceeded.  $A_{0.01}$  represents the attenuation exceeded for 0.01% of the time and it depends on the station meteorology, path elevation, and frequency of the Earth-space radio link. To show numerical examples we have considered a particular link at 30 GHz for which  $A_{0.01}$  turns out to be 28.5 dB. Clearly the higher the value of the factor  $\alpha \beta$ , the higher the amount of back-up capacity needed to provide the required availability. In the example considered above ( $N=50$  stations and  $\alpha \beta = 15$ ) it turns out from equation (3) that for a link at 30 GHz with  $p = 5 \times 10^{-3}$  the outage probability with frequency diversity is less than  $2 \times 10^{-4}$  if a reserve capacity of  $k = 6$  is used. In this case the link is designed with a power margin corresponding to  $p = 5 \times 10^{-3}$ , that is 4.9 dB. To obtain the same outage results without frequency diversity protection, a power margin of 21.7 dB is needed according to equation (4). Notice that the power margin needed without frequency diversity is remarkable. Besides the increased costs of the link, this very high extra power may also cause interference with other radio links.

FIGURE 6

Outage reduction factor  $G$  versus number of back-up channels  $k$ 

$p$  : outage probability without frequency diversity

### 5.3 Operation of adaptive control system and simulation results

The previous analysis of the performance of frequency diversity systems was performed for the ideal case, in which switching from the normal mode to the assisted mode (and *vice versa*) can be made instantaneously. In a real adaptive fade countermeasure system the response time is not negligible especially when assignment on demand of back-up capacity is used; the delay in setting up the fade countermeasure or in restoring the initial condition is mainly due to the propagation through the space link (from a terminal to the master station and back) and depends on the protocol used.

An adaptive fade countermeasure system to detect fades requires measuring the instantaneous conditions of the channel by directly monitoring the attenuation or by estimating the bit error rate. Because of the set-up delay of the fade countermeasure system, the system should take into account the dynamic characteristics of fading, in particular its rate of change and the presence of fast fluctuations, in order to predict in advance the crossing of the attenuation level  $S$ , corresponding to the minimum acceptable quality, and to be able to set-up in due time the fade countermeasure.

The simplest way to do this is to initiate the set-up procedure when the attenuation reaches the level  $S_1 = S - M$ ,  $M$  being a suitable margin chosen in relation to the statistical attenuation rate of change. As far as the attenuation rate of change is concerned, some experimental data have been reported for the 14/11 GHz band.

To avoid outage conditions during set-up time,  $M$  should be chosen large enough; on the other hand, a too-large value for  $M$  may result in an inefficient use of the fade countermeasure. The occurrence of false alarms implies that the shared resource will be used for longer than necessary, and this may cause outage conditions in the case of simultaneous requests of back-up capacity.

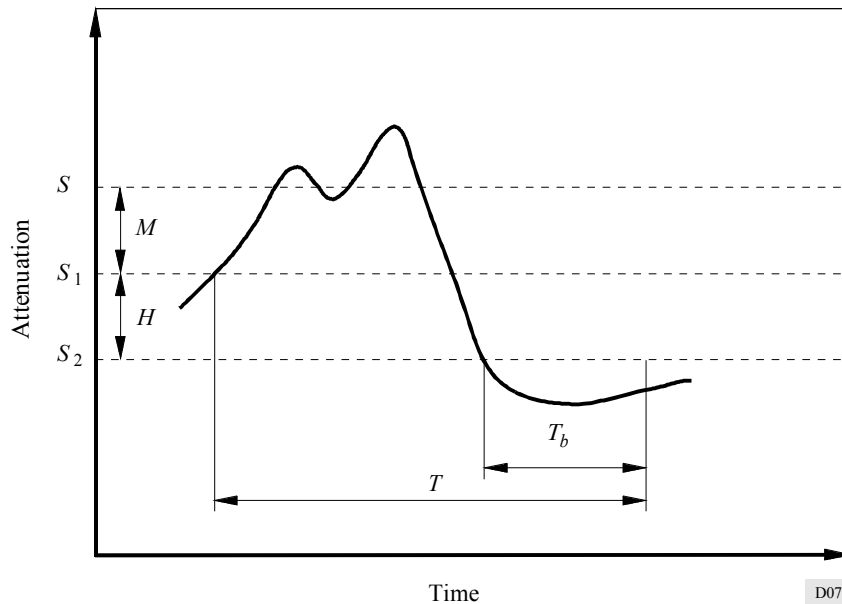
The performance of this switchover procedure has been analysed and compared with the performance obtained by predicting the attenuation level on the basis of the previous attenuation samples. Algorithms for real-time prediction of rain attenuation based on linear regression have been investigated. While the regression algorithm can predict the average trend of attenuation, it cannot predict the very fast fluctuations of fading. So the results presented have been obtained by

implementing the regression algorithm on different numbers of previous samples and adding to the value predicted a constant offset to counteract the very fast fluctuations. The parallel line passing through the last sample is considered in addition to the regression line because it improves the performance of prediction.

The presence of relatively fast fluctuations of attenuation should also be carefully considered in choosing the procedure to switch off the fade countermeasure, when fading conditions disappear. In practice it may be convenient to filter out the attenuation oscillations by maintaining the system in the protected conditions (fade countermeasure on) while the attenuation is fluctuating around the threshold  $S_1 = S - M$ . The margin against fast fluctuations is represented by  $M$ , in the case of the regression algorithm. A solution is to introduce a hysteresis  $H$ , namely to switch off the fade countermeasure when the attenuation falls below the level  $S_2 = S_1 - H$ . In order to have an additional protection against fast fluctuations, the switching off of the fade countermeasure can be delayed for an interval  $T_b$  suitably chosen. The switching off is actuated only if the attenuation constantly remains below  $S_2$  during the interval  $T_b$  (Fig. 7). The solution of introducing a margin  $M$  in switching on and a hysteresis  $H$  and a delay  $T_b$  in switching off implies a reduction in the efficiency of the system with respect to the system with ideal control, where  $M = H = T_b = 0$ , because the reserve capacity is used by the faded link for a longer time.

FIGURE 7

Definition of parameters which characterize switchover procedure between normal mode and assisted mode, or vice versa



To analyse and compare the performance of the different control systems, two parameters have been considered. The first one is the percentage of occurrences of outage conditions during set-up time, with respect to the number of times the fade countermeasure was provided to the faded link. The second one is the efficiency of the system, defined by the utilization factor  $U = (T_{tot} - T_{ideal}) / T_{ideal}$ , where  $T_{tot}$  is the total utilization time of the back-up capacity in the system and  $T_{ideal}$  is the utilization time of the back-up capacity in a system with ideal control.

The system behaviour was simulated using the attenuation time series at 11.6 GHz measured with the Sirio satellite throughout four years (from 1979 to 1982) at a station in Spino d'Adda, northern Italy. The statistical results obtained are reliable, because the amount of experimental data available was very large.

Though the analysis of the switchover procedure is based on attenuation time series at 11.6 GHz, the simulation results obtained are also a good estimate of the statistical performance of the switchover at 20 and 30 GHz, as discussed below.

When experimental results concerning rain attenuation are extrapolated from lower frequencies to higher frequencies, at least two phenomena should be considered: the attenuation due to the hydrometeors and the scintillation due to multipath propagation (associated with rapid variations of the equivalent index of refraction produced by the air and hydrometeor scattering).

The extrapolation of measured rain attenuation has been investigated and good extrapolation formulae are now available. As attenuation and scintillation occurring at one frequency are not separated in the extrapolated data, these empirical formulae extrapolate the effects of both phenomena to a higher frequency.

A real-time frequency extrapolation is not currently available, however, the switchover statistical results can only be extrapolated at fixed 11.6 GHz thresholds to the corresponding thresholds at 20 or 30 GHz. It may be evident that these results, statistically, are also valid at these higher frequencies. In fact these frequencies are not so high that they show unexpected physical phenomena, according to the few results known up to now. The physical foundations of rain attenuation are very well known and the experiments agree well with predicted long-term attenuation statistics. Also the physical foundations of the clear or "wet" air scintillation are theoretically well known and the models are experimentally confirmed. Experimental results on scintillation power spectra at 11.6 GHz, can be extrapolated by simple models to higher frequencies. For instance, considering the dimensions of the antennas and the frequencies of a frequency diversity experiment planned with the European satellite Olympus, the average scintillation power spectrum decreases with the frequency  $f$  according to the theoretical law  $f^{-8/3}$ , starting from about 0.5 Hz at 20 GHz and about 0.6 Hz at 30 GHz; these data become, respectively, 1.6 Hz and 2 Hz in 95% of the cases. At 12.5 GHz, the corresponding frequencies are about 0.4 Hz and 1.3 Hz.

The amplitude of the scintillations, statistically, increases much less than the rain attenuation. The standard deviation of the scintillation, for a given path and identical physical conditions, increase only as  $f^{7/12}$ , while rain attenuation increases, roughly, as  $f^{1.76}$ . As a consequence it is also expected that the overall dynamic behaviour at 20 and 30 GHz is not very different from that measured at 11.6 GHz, once attenuation thresholds are scaled up.

#### 5.4 Simulation results

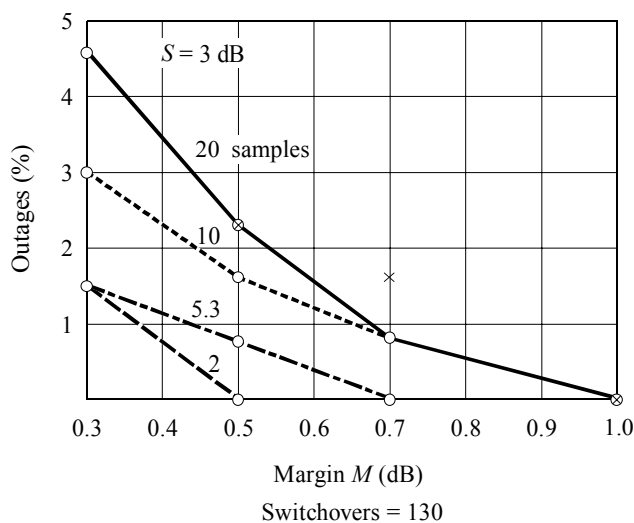
In order to compare the percentage of outages during set-up time of the different control procedures on the basis of the same number of switchover procedures performed, the threshold  $S_2$  of switching off has been kept constant. Figures 8 and 9 show the results of the simulations performed considering outage threshold  $S = 3$  dB, set-up delay  $T_c = 2$  s, threshold of switching off  $S_2 = 1.8$  dB, and interval  $T_b = 20$  s. The outage threshold  $S$  chosen is that one exceeded at about  $10^{-3}$  probability at 11.6 GHz at Spino d'Adda, which corresponds to about 8 dB at 20 GHz.

The prediction algorithm is based on the past 20, 10, 5, 3 and 2 samples and utilizes a margin against fast fluctuations equal to 0.3 dB, 0.5 dB, 0.7 dB, or 1 dB. If the attenuation level, predicted with an anticipation time equal to 2 s (the set-up delay) plus a guard time of 1 s (the attenuation sampling frequency), exceeds the threshold  $S$ , the set-up procedure is initiated. For the algorithm utilizing the fixed pre-threshold,  $S_1$  has been considered equal to 2.5 dB, 2.3 dB and 2 dB, that correspond to an allowable attenuation rate of change of 0.25 dB/s, 0.35 dB/s and 0.5 dB/s.

The results suggest that the system implementing the fixed pre-threshold algorithm presents about the same performance as the system implementing the prediction based on the past 20 samples. Concerning the percentage of outages, the best performance is reached implementing the prediction of attenuation from only the past two samples and adding a margin against scintillation of 0.5 dB. It is evident that, on the contrary, reducing the number of previous samples used for prediction, the utilization time of the fade countermeasure increases, since more false alarms may occur. The factor  $U$  increases up to about 1.2, meaning that the fade countermeasure utilization time is more than twice the total utilization time in the ideal case. If the back-up capacity available is small and the number of earth stations that share it is large, it could be convenient to implement the algorithm that improves the efficiency of the system, even if it increases the number of short outages during set-up time. Large utilization times of the fade countermeasure are also due to the large value of hysteresis  $H$  (0.7 dB) and of delay  $T_b$  (20 s), introduced in the procedure to restore the normal transmission conditions. Figure 10 shows the results of the simulations performed to evaluate the effect of reducing the delay  $T_b$ , initially fixed to 20 s. The prediction algorithm has been implemented using only the past two samples, and considering a margin against fluctuations of 0.5 dB and a hysteresis  $H = 0.2$  dB. It can be noted that this value of hysteresis and a delay  $T_b$  equal to 10 s are sufficient to counteract efficiently the fast fluctuations, decreasing the factor  $U$  from 1.2 to 0.8.

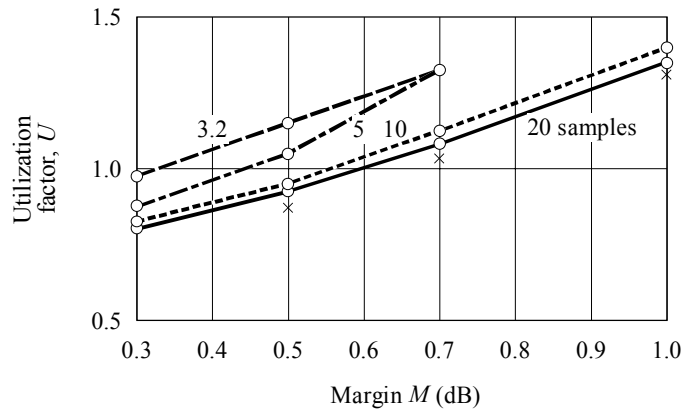
FIGURE 8

Percentage of outages expected during set-up time versus anticipation margin



Points marked with x show results when a fixed pre-threshold algorithm is implemented. Other curves show the results when a linear prediction algorithm is implemented with the indicated number of previous samples.

FIGURE 9  
Utilization factor  $U$  versus anticipation margin

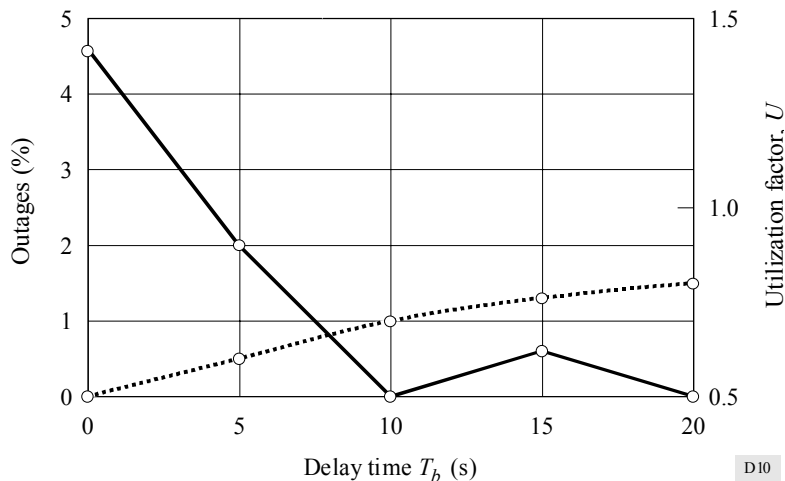


Points marked with x show results when a fixed pre-threshold algorithm is implemented. Other curves show the results when a linear prediction algorithm is implemented with the indicated number of previous samples.

D09

The simulation results show that the nature of the attenuation time evolution during rain events is such that good prediction methods are difficult to devise. The simplest and more robust technique seems to be a fixed anticipation margin of suitable amplitude. The prediction algorithms here examined cannot significantly improve the overall performance (measured by the number of outages and by the utilization factor) compared with that using the fixed anticipation margin. In any case it is always possible to trade-off the number of outages (i.e. the quality) with the amount of the utilization factor (i.e. the availability). Of course, this trade-off depends on the particular communication system requirements.

FIGURE 10  
Percentage of outages during set-up time (continuous line) and utilization factor  $U$  (dashed line) versus delay time  $T_b$ . The linear prediction is based on the previous two samples and the margin against fluctuations is 0.5 dB



D10



## 5.5 Conclusion

The method of dual-band frequency diversity is particularly effective when low levels of outage probability are required.

Dual-band frequency diversity provides large equivalent power margins with a limited amount of back-up capacity available. The number of back-up channels needed depends also on the correlation properties of the attenuation processes relative to the different sites of the stations.

---